PHYSICAL REVIEW B **87**, 100403(R) (2013)

Determination of long-range all-in-all-out ordering of Ir^{4+} moments in a pyrochlore iridate $Eu_2Ir_2O_7$ by resonant x-ray diffraction

H. Sagayama,[1] D. Uematsu,[1] T. Arima,[1,2] K. Sugimoto,[3] J. J. Ishikawa,[4] E. O'Farrell,[4] and S. Nakatsuji[4]

[1]*Department of Advanced Materials Science, The University of Tokyo, 5-1-5 Kashiwanoha, Kashiwa, Chiba 277-8561, Japan*

[2]*RIKEN SPring-8 Center, 1-1-1 Kouto, Sayo-cho, Sayo-gun, Hyogo 679-5148, Japan*

[3]*Japan Synchrotron Radiation Research Institute (JASRI), SPring-8, 1-1-1 Kouto, Sayo-cho, Sayo-gun, Hyogo 679-5198, Japan*

[4]*Institute for Solid State Physics, The University of Tokyo, 5-1-5 Kashiwanoha, Kashiwa, Chiba 277-8581, Japan*

(Received 10 September 2012; revised manuscript received 6 December 2012; published 18 March 2013)

The pyrochlore-type iridium oxide $Eu_2Ir_2O_7$ exhibits a metal-insulator transition at 120 K, accompanied by magnetic ordering. We used x-ray diffraction measurements with photon energies near the iridium L_3 absorption edge to analyze a single crystal to investigate the arrangement of Ir^{4+} magnetic moments. Resonant magnetic scattering at $(4n + 2\,0\,0)$ was observed in the insulating phase, providing direct evidence of long-range ordering of Ir^{4+} magnetic moments with a propagation vector of $\boldsymbol{q} = (000)$. Our single-crystal structure analysis revealed that the lattice retains its face-centered-cubic structure across the metal-insulator transition, indicating all-in-all-out magnetic order, where all the magnetic moments on the four vertices of each Ir tetrahedron point inward or outward.

DOI: 10.1103/PhysRevB.87.100403 PACS number(s): 75.25.−j, 61.05.cp, 75.47.Lx, 75.50.Ee

Magnetic compounds with a pyrochlore structure show a variety of properties, such as a metal-insulator (M-I) transition, superconductivity, the spin-ice state, and the spin-chirality-driven anomalous Hall effect.[1] The pyrochlore structure exhibits geometrical frustration, which arises from the tetrahedral network. As a result, nontrivial states may be present in magnetic systems that contain the pyrochlore lattice. For example, $Tl_2Ru_2O_7$ undergoes a cubic-orthorhombic structural transition at 120 K, below which the spin gap is formed.[2,3] $Hg_2Ru_2O_7$ also exhibits a structural transition, and a commensurate antiferromagnetic order has been proposed.[4–6] However, the cubic symmetry in $Cd_2Os_2O_7$ is not broken across the M-I transition, and the four-sublattice noncoplanar magnetic order, called the all-in-all-out structure, has recently been reported.[7]

The M-I transition of a series of pyrochlore iridate, $R_2Ir_2O_7$, where R is a trivalent rare earth, has also been investigated. The interplay between the electron correlation and the spin-orbit interaction in a tetrahedral network of 5d transition metal ions was investigated by systematically replacing R. The compounds where R = Y, Yb, Ho, Dy, Tb, Gd, Eu, Sm, or Nd exhibit the M-I transition, accompanying a magnetic anomaly.[8–11] As the ionic radius of R increases, the M-I transition temperature T_{MI} decreases and finally approaches zero between Nd and Pr.[11] The electrical conductivity in the high-temperature paramagnetic phase also increases with the ionic radius of R. In $R_2Ir_2O_7$, the 5d state of Ir is split into the lower-lying triplet t_{2g} states and the higher-lying doublet e_g states by an octahedral ligand field. The t_{2g} state is partially filled by five electrons, which produces a magnetic moment. A spin-glass-like state in the insulator phase has been proposed, based on the difference in magnetization between the zero-field-cooling and field-cooling processes.[8] However, a clear λ peak in the temperature dependence of the heat capacity has been reported at the T_{MI} in a high-quality polycrystalline sample, suggesting a second-order transition.[10–12]

The strong spin-orbit coupling in the Ir pyrochlore is also particularly interesting. Some theoretical studies suggest that exotic quantum states could behave as topological Mott insulators and Weyl semimetals.[13–16] Although the magnetic structure in the insulating phase is a fundamental factor in determining the electronic state, it still needs to be experimentally determined. For example, the Weyl semimetal state is expected to appear when the time-reversal symmetry is broken.[15] A muon spin rotation study revealed a spontaneous local field below T_{MI} for R = Y, Eu, and Yb, which indicates some long-range commensurate magnetic ordering.[17,18] Tomiyasu *et al.* determined the arrangement of Nd moments by neutron diffraction measurements and proposed that the Ir^{4+} moments should form the all-in-all-out structure [Fig. 1(a)].[19] Nonetheless, no direct evidence of the ordered Ir^{4+} moments has been obtained from neutron diffraction studies for R = Nd (Refs. 19 and 20) and Y,[18,21] because of the high absorption of neutrons by Ir atoms and the small ordered moments.

We have used resonant x-ray diffraction (RXD) to determine the magnetic structure of $Er_2Ir_2O_7$. RXD is a useful technique for studying magnetic order in 5d transition metal compounds,[22,23] because the $L_{2,3}$ absorption edges correspond to x-ray wavelengths of ∼1 Å, which are short enough for a diffraction study. The magnetic reflections are expected to show a large resonance enhancement, because the $L_{2,3}$ excitations are relevant to the 5d states with a magnetic moment.

Single crystals of $Eu_2Ir_2O_7$ were grown by the flux method.[24] The electrical conductivity is affected by the off stoichiometry in the ratio of Eu to Ir.[12] The resistivity ρ was measured by the four-probe method from 300 to 2 K on several single crystals. A high-quality crystal with an inverse resistivity ratio of $\rho(2\text{ K})/\rho(300\text{ K}) = 7600$ was selected for the RXD measurement performed by using a seven-circle diffractometer installed at BL3A, Photon Factory, High Energy Accelerator Research Organization, Japan. The energy of the incident x rays was tuned to around the Ir L_3 absorption edge, 11.23 keV, with a Si (111) double-crystal monochromator. The incident x ray was linearly polarized perpendicular to the scattering plane (σ). The sample with a flat triangular (111)

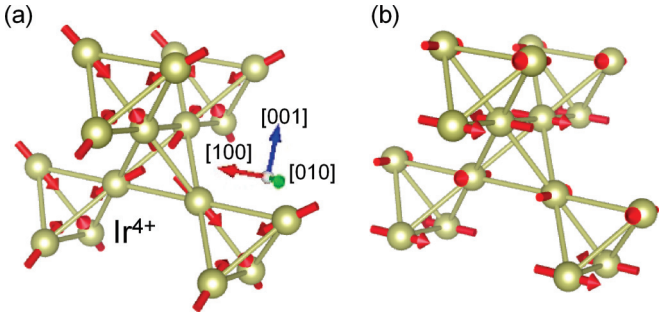

FIG. 1. (Color online) (a) All-in-all-out magnetic structure where all four magnetic moments on the vertices of each tetrahedron point inward or outward. Arrows indicate the Ir^{4+} magnetic moments. (b) Coplanar magnetic order where four magnetic moments on a tetrahedron lie in the (001) plane and are either antiparallel or orthogonal.

surface with edges about 0.5 mm long [Fig. 2(b)] was attached to a copper plate with varnish and mounted in a closed-cycle ^{4}He refrigerator. The [011] of the sample was oriented perpendicular to the scattering plane [Fig. 2(a)]. A Mo (200) crystal was used to analyze the polarization of the scattered x ray. The linearly polarized σ' (perpendicular to the scattering plane) and π' (parallel to the scattering plane) components can be detected by rotating the Mo crystal about the scattered beam. The 2θ value of the (200) reflection of Mo is 89.564° at 11.230 keV, which guarantees a polarization purity of 99.99%. To investigate the change in crystal structure across the M-I transition, x-ray oscillation photographs were taken with a large cylindrical imaging plate installed at BL02B1, SPring-8, Japan, at a photon energy of 35 keV, which is far from the absorption edges of the constituent elements.[25] A single crystal sample with a dimension of 0.05 mm was cooled by using a He-gas spray refrigerator. SHELXL (Ref. 26) was used to refine the structural parameters. The magnetic susceptibility of three single crystals (0.49 mg), including the one used for the RXD

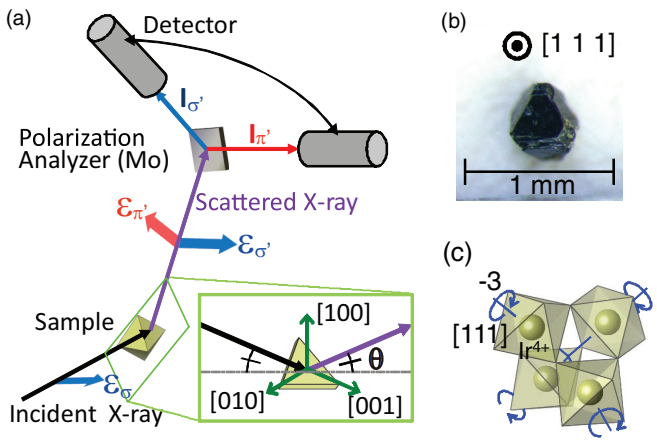

FIG. 2. (Color online) (a) Schematic view of the experimental setup for the resonant magnetic x-ray diffraction measurements. (b) Photograph of the $Eu_2Ir_2O_7$ single crystal used for the RXD experiment. (c) Ir-O network in the pyrochlore structure. Each Ir is coordinated to six O atoms. The IrO_6 octahedra are connected by shared vertices to form a tetrahedral Ir network. Each IrO_6 is compressed along a trigonal axis.

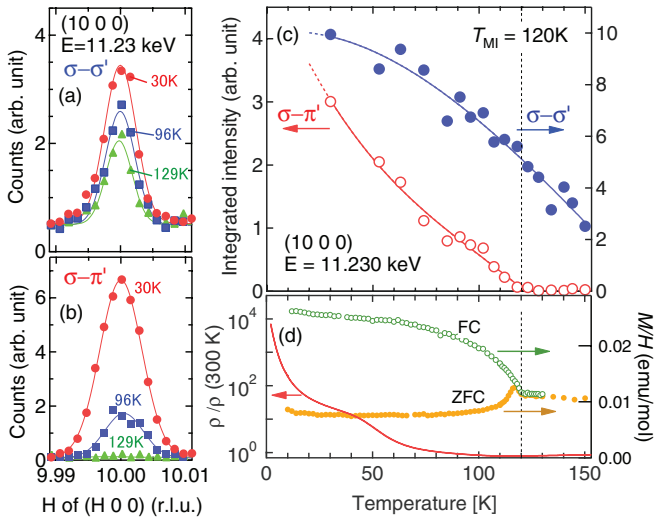

FIG. 3. (Color online) (a), (b) Profiles of the (1000) reflections of $Eu_2Ir_2O_7$ scanned along (h00) in reciprocal space with a photon energy of 11.230 keV at several temperatures through the (a) σ-σ' and (b) σ-π' channels. (c) Temperature dependence of the integrated intensities of the (1000) reflection detected though the σ-σ' (solid circles) and σ-π' (open circles) channels. (d) Temperature dependence of the electrical resistivity (solid line) and magnetic susceptibility (circles). The magnetic susceptibilities were measured for zero-field-cooling (ZFC; solid circles) and field-cooling (FC; open circles) processes in a field of 1000 Oe.

measurement (0.3 mg), was measured with a superconducting quantum interference device magnetometer under an applied magnetic field of 1000 Oe.

Initially, several line scans were performed along (h00), (hh0), and (hhh) in the reciprocal space to search for magnetic reflections with the on-resonance condition. No reflections at incommensurate positions were observed (not shown). Forbidden reflections at $(4n+2\,0\,0)$ were then investigated. In pyrochlore systems with an $Fd\bar{3}m$ space group, the (h00) reflections are allowed only when $h=4n$, where n is an integer. Figures 3(a) and 3(b) show the x-ray diffraction profiles for the σ-σ' and σ-π' channels along (h00) around $h=10$ at a photon energy of 11.230 keV and at several temperatures. A clear peak was observed at (1000) in both the polarization channels. The integrated intensity of the peak is plotted as a function of temperature (Fig. 3). The reflection in the σ-π' channel appeared only below $T_{MI}=120$ K. The intensity in the σ-π' channel ($I_{\sigma\text{-}\pi'}$) below the T_{MI} increased approximately linearly to $T_{MI}-T$, which is consistent with a second-order phase transition. In contrast, the peak was also visible above T_{MI} in the σ-σ' channel. In the resonance condition, $(4n+2\,0\,0)$ reflections can arise from the anisotropy of the anomalous scattering factor of Ir^{4+} ions. The Ir^{4+} ions occupy trigonally distorted octahedral sites with a local symmetry of $\bar{3}m$, which causes the uniaxial anisotropy in the anomalous scattering factor tensor with the spatial axis parallel to the trigonal axis.[27] Because the special axes for the four Ir sites in the primitive cell are not parallel to each other [Fig. 2(c)], the reflection condition is relaxed near the Ir absorption edges.[28] The [011] axis was set perpendicular to the scattering plane; therefore the structure factors of the $(4n+2\,0\,0)$ reflections in the σ-σ'

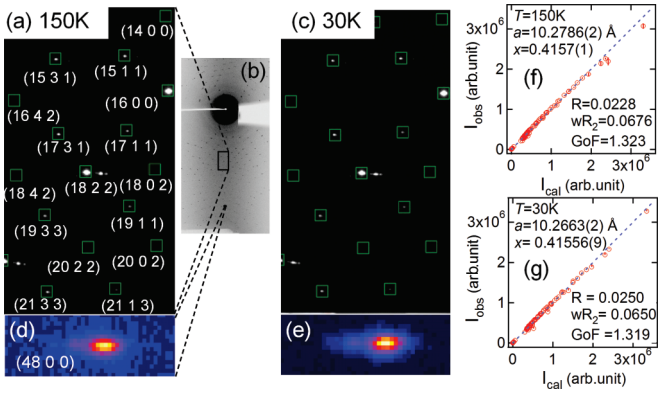

FIG. 4. (Color online) X-ray oscillation photographs of $Eu_2Ir_2O_7$. Closeup pictures of two areas at (a), (d) 150 K and (c), (e) 30 K. Comparisons of the observed (I_{obs}) and calculated (I_{cal}) intensities of the reflections at (f) 150 K and (g) 30 K, where x is the coordinate of the oxygen occupying the 48f site.

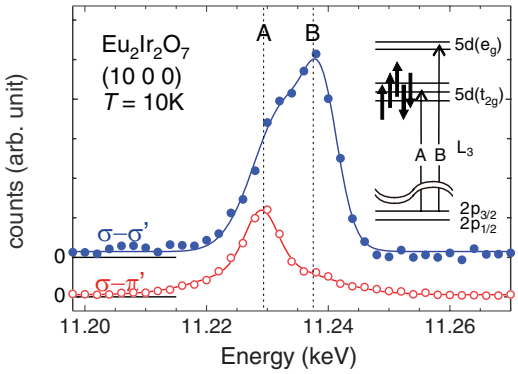

FIG. 5. (Color online) Spectra of the intensity of the (10 0 0) reflection around the Ir L_3 edge in the σ-σ' and σ-π' channels. The inset shows an energy level scheme of the Ir^{4+} 5d orbital, which is raised by the occupied octahedral ligand field. The long arrows show the electron excitation processes for the L_3 absorption edge. "A" and "B" denote the excitation from $2p_{3/2}$ to t_{2g} and that from $2p_{3/2}$ to e_g, respectively.

and σ-π' processes are

$$F_{\sigma\sigma'} \propto \frac{16}{3}(f_\perp - f_\parallel) \tag{1}$$

and

$$F_{\sigma\pi'} = 0, \tag{2}$$

respectively. Here $f_\perp$ and $f_\parallel$ are the anomalous anisotropic scattering factors perpendicular and parallel to the local trigonal axis, respectively. Thus, the $(4n + 2\,0\,0)$ reflections in σ-σ' arose from the local anisotropy at the Ir sites. The gradual change in $I_{\sigma\text{-}\sigma'}$ with temperature was probably caused by a change in the population of the 5d electron bands (orbitals) through the thermal excitation.

Equation (2) implies that the (10 0 0) reflection in the σ-π' channel can be assigned to the magnetic scattering, if the crystallographic symmetry is unchanged across the M-I transition. The symmetry above and below T_{MI} was examined using a high-quality single crystal. Figure 4 shows oscillation photographs taken at 30 and 150 K. The reflection condition was unchanged [Figs. 4(a) and 4(c)], and the (48 0 0) reflection remained as a single peak with no splitting [Figs. 4(d) and 4(e)], indicting no lattice distortion through the M-I transition.[29] The crystal structures at 30 and 150 K were analyzed using the $Fd\bar{3}m$ space group with an accuracy of $R = 2.50\%$ and 2.28%, respectively. All the parameters, residuals, and goodness of fit indicators are listed in the Supplemental Material.[30] The crystal structure of a regular pyrochlore compound contains only one free parameter: the atomic coordinate x of the anion sites. In our analysis, $x = 0.415\,56(9)$ at 30 K and 0.4157(1) at 150 K, indicating the crystal structure was unchanged. Therefore the $(4n + 2\,0\,0)$ reflections in the σ-π' process were assigned to magnetic scattering. A previous Raman study suggested that the symmetry could be lowered at low temperatures.[31] However, the study also found there was no splitting of the t_{2g}-mode phonons, indicating that the cubic symmetry should not be violated.

Figure 5 shows that the σ-σ' and σ-π' spectrum of the (10 0 0) reflection. The trigonal distortion of the octahedral field makes the transition probabilities from the $2p_{3/2}$ core to the t_{2g} and e_g states anisotropic, and thus induces the resonant enhancement for both. As the magnetism of the iridate compound is predominated by the partially filled t_{2g} but not by the empty e_g state, magnetic scattering may not be resonant with the $2p$-e_g excitation. The absence of a resonant enhancement around 11.238 keV in the (10 0 0) $I_{\sigma\text{-}\pi'}$ spectrum is consistent with its magnetic origin.

It was predicted that the Dzyaloshinskii-Moriya interaction could eliminate the geometrical spin frustration in the pyrochlore lattice and consequently stabilize the all-in-all-out or coplanar arrangement of magnetic moments (Fig. 1).[32] For the all-in-all-out arrangement, the intensity of the resonant magnetic scattering for (10 0 0) through the σ-π' channel can be expressed as

$$I_{\sigma\text{-}\pi'} \propto \frac{m^2}{3}\sin^2\theta, \tag{3}$$

where m is the Ir magnetic moment, and θ is the incident angle. Meanwhile, the (10 0 0) reflection for the coplanar arrangement, with moments in the (011) and (010) planes, can also be expressed using Eq. (3), although the magnetic peak does not appear when the moments lie in the (100) plane. The magnetic scattering alone cannot determine the magnetic structure.

Magnetic ordering could cause lattice distortion through the exchange striction. In $ZnCr_2O_4$, where Cr^{3+} ions form the pyrochlore lattice, a structural transition occurs. The transition is driven by commensurate long-range spin ordering, where spin and lattice degrees of freedom couple through the inverse effects of the exchange interaction and the Dzyaloshinskii-Moriya interaction.[33] Iridium oxides are expected to show even larger magnetostriction because of the strong spin-orbit interaction and the spatial extension of the 5d orbitals. Hereafter we discuss the magnetic structure in terms of its irreducible representation.[34] For the pyrochlore lattice with magnetic propagation vector, $\boldsymbol{q} = (000)$, the basis functions consist of one singlet (Γ_3), one doublet (Γ_5), and three triplets (Γ_7 and two sets of Γ_9). All the magnetic structures should give

rise to some structural distortion, apart from Γ_3, which is the all-in-all-out structure, because only the all-in-all-out structure belongs to the symmetric A_g group. Our crystal structure analysis indicates there is no crystallographic symmetry breaking and hence suggests the all-in-all-out magnetic order in the insulating phase of $Eu_2Ir_2O_7$.

The correlation length of the magnetic ordering was estimated from the (1 0 0 0) peak profiles fitted using the Gaussian function. The q resolution was estimated from the peak profile in the σ-σ' channel and the essential width of the magnetic peak was deconvoluted from this data. The net value of the half width at half maximum of the magnetic reflection was 0.00214 in the reciprocal lattice unit. The magnetic correlation length was estimated to be ∼4800 Å at 30 K.

The authors thank H. Nakao and Y. Yamasaki for their support at Photon Factory. This work was supported in part by Grants-in-Aid for Scientific Research No. 19052001 and No. 24224010 from MEXT, Japan, and the Funding Program for World Leading Innovative R&D on Science and Technology (FIRST) on "Quantum Science on Strong Correlation" from the Japan Society for the Promotion of Science.

[1] J. S. Gardner, M. J. P. Gingras, and J. E. Greedan, Rev. Mod. Phys. **82**, 53 (2010).
[2] T. Takeda, R. Kanno, Y. Yamamoto, M. Takano, F. Izumi, A. W. Sleight, and A. W. Hewar, J. Mater. Chem. **9**, 215 (1999).
[3] S. Lee, J.-G. Park, D. T. Adroja, D. Khomskii, S. Streltsov, K. A. McEwen, H. Sakai, K. Yoshimura, V. I. Anisimov, D. Mori, R. Kanno, and R. Ibberson, Nat. Mater. **5**, 471 (2006).
[4] W. Klein, R. K. Kremer, and M. Jansen, J. Mater. Chem. **17**, 1356 (2007).
[5] A. Yamamoto, P. A. Sharma, Y. Okamoto, A. Nakao, H. A. Katori, S. Niitaka, D. Hashizume, and H. Takagi, J. Phys. Soc. Jpn. **76**, 043703 (2007).
[6] M. Yoshida, M. Takigawa, A. Yamamoto, and H. Takagi, J. Phys. Soc. Jpn. **80**, 034705 (2011).
[7] J. Yamaura, K. Ohgushi, H. Ohsumi, T. Hasegawa, I. Yamauchi, K. Sugimoto, S. Takeshita, A. Tokuda, M. Takata, M. Udagawa, M. Takigawa, H. Harima, T. Arima, and Z. Hiroi, Phys. Rev. Lett. **108**, 247205 (2012).
[8] N. Taira, M. Wakeshima, and Y. Hinatsu, J. Phys.: Condens. Matter **13**, 5527 (2001).
[9] D. Yanagishima and Y. Maeno, J. Phys. Soc. Jpn. **70**, 2880 (2001).
[10] K. Matsuhira, M. Wakeshima, R. Nakanishi, T. Yamada, A. Nakamura, W. Kawano, S. Takagi, and Y. Hinatsu, J. Phys. Soc. Jpn. **76**, 043706 (2007).
[11] K. Matsuhira, M. Wakeshima, Y. Hinatsu, and S. Takagi, J. Phys. Soc. Jpn. **80**, 094701 (2011).
[12] J. J. Ishikawa, E. C. T. O'Farrell, and S. Nakatsuji, Phys. Rev. B **85**, 245109 (2012).
[13] D. Pesin and L. Balents, Nat. Phys. **6**, 376 (2010).
[14] B.-J. Yang and Y. B. Kim, Phys. Rev. B **82**, 085111 (2010).
[15] X. Wan, A. M. Turner, A. Vishwanath, and S. Y. Savrasov, Phys. Rev. B **83**, 205101 (2011).
[16] W. Witczak-Krempa and Y. B. Kim, Phys. Rev. B **85**, 045124 (2012).
[17] S. Zhao, J. M. Mackie, D. E. MacLaughlin, O. O. Bernal, J. J. Ishikawa, Y. Ohta, and S. Nakatsuji, Phys. Rev. B **83**, 180402(R) (2011).
[18] S. M. Disseler, C. Dhital, A. Amato, S. R. Giblin, C. de la Cruz, S. D. Wilson, and M. J. Graf, Phys. Rev. B **86**, 014428 (2012).
[19] K. Tomiyasu, K. Matsuhira, K. Iwasa, M. Watahiki, S. Takagi, M. Wakeshima, Y. Hinatsu, M. Yokoyama, K. Ohoyama, and K. Yamada, J. Phys. Soc. Jpn. **81**, 034709 (2012).
[20] S. M. Disseler, C. Dhital, T. C. Hogan, A. Amato, S. R. Giblin, C. de la Cruz, A. Daoud-Aladine, S. D. Wilson, and M. J. Graf, Phys. Rev. B **85**, 174441 (2012).
[21] M. C. Shapiro, S. C. Riggs, M. B. Stone, C. R. de la Cruz, S. Chi, A. A. Podlesnyak, and I. R. Fisher, Phys. Rev. B **85**, 214434 (2012).
[22] D. F. McMorrow, S. E. Nagler, K. A. McEwen, and S. D. Brown, J. Phys.: Condens. Matter **15**, L59 (2003).
[23] B. J. Kim, H. Ohsumi, T. Komesu, S. Sakai, T. Morita, H. Takagi, and T. Arima, Science **323**, 1329 (2009).
[24] J. N. Millican, R. T. Macaluso, S. Nakatsuji, Y. Machida, Y. Maeno, and J. Y. Chan, Mater. Res. Bull. **42**, 928 (2007).
[25] K. Sugimoto, H. Ohsumi, S. Aoyagi, E. Nishibori, C. Moriyoshi, Y. Kuroiwa, H. Sawa, and M. Takata, in *SRI 2009, 10th International Conference on Synchrotron Radiation Instrumentation*, edited by R. Garrett *et al.*, AIP Conf. Proc. Vol. 1234 (AIP, Melville, NY, 2010), p. 887.
[26] G. M. Sheldrick, Acta Crystallogr. Sect. A **64**, 112 (2008).
[27] D. H. Templeton and L. K. Templeton, Acta Crystallogr. Sect. A **38**, 62 (1982).
[28] V. E. Dmitrienko, Acta Crystallogr. Sect. A **39**, 29 (1983).
[29] If the lattice was tetragonally distorted, for example, we could find a split or broadening of the (48 0 0) reflection profile. The upper limit to possible lattice distortion $(a_t - c_t)/a_t$ is 0.0004 in this experimental accuracy, where a_t and c_t are lattice constants.
[30] See Supplemental Material at http://link.aps.org/supplemental/10.1103/PhysRevB.87.100403 for the present crystal-structure analyses.
[31] T. Hasegawa, N. Ogita, K. Matsuhira, S. Takagi, M. Wakeshima, Y. Hinatsu, and M. Udagawa, J. Phys.: Conf. Ser. **200**, 012054 (2010).
[32] M. Elhajal, B. Canals, R. Sunyer, and C. Lacroix, Phys. Rev. B **71**, 094420 (2005).
[33] S. Ji, S.-H. Lee, C. Broholm, T. Y. Koo, W. Ratcliff, S. W. Cheong, and P. Zschack, Phys. Rev. Lett. **103**, 037201 (2009).
[34] Y. A. Izyumov, V. E. Naish, and R. P. Ozerov, *Neutron Diffraction of Magnetic Materials* (Plenum, New York, 1991).